Eleonorite, $Fe_6^{3+}(PO_4)_4O(OH)_4 \cdot 6H_2O$: validation as a mineral species and new data

NIKITA V. CHUKANOV[1,*], SERGEY M. AKSENOV[2,3], RAMIZA K. RASTSVETAEVA[3], CHRISTOF SCHÄFER[4], IGOR V. PEKOV[5], DMITRIY I. BELAKOVSKIY[6], RICARDO SCHOLZ[7], LUIZ C.A. DE OLIVEIRA[8] AND SERGEY N. BRITVIN[3]

[1] Institute of Problems of Chemical Physics, Russian Academy of Sciences, Chernogolovka, Moscow region, 142432 Russia

[2] Faculty of Geology, St Petersburg State University, University Embankment 7/9, St Petersburg, 199034 Russia

[3] Institute of Crystallography, Russian Academy of Sciences, 59 Lenin Avenue, Moscow, 117333 Russia

[4] Südwestdeutsche Salzwerke AG, Salzgrund 67, 74076 Heilbronn, Germany

[5] Faculty of Geology, Moscow State University, Vorobievy Gory, Moscow, 119991 Russia

[6] Fersman Mineralogical Museum of the Russian Academy of Sciences, Leninsky Prospekt 8-2, Moscow, 117071 Russia

[7] Universidade Federal de Ouro Preto (UFOP), Escola de Minas, Departamento de Geologia, Campus Morro do Cruzeiro, 35400-000, Ouro Preto, MG, Brazil

[8] Universidade Federal de Minas Gerais, Instituto de Ciências Exatas, Departamento de Química, Avenida Antônio Carlos, 6627, 31270-901, Belo Horizonte, MG, Brazil

ABSTRACT

Eleonorite, ideally $Fe_6^{3+}(PO_4)_4O(OH)_4 \cdot 6H_2O$, the analogue of beraunite $Fe^{2+}Fe_5^{3+}(PO_4)_4(OH)_5 \cdot 6H_2O$ with Fe^{2+} completely substituted by Fe^{3+}, has been approved by the International Mineralogical Association Commission on New Minerals, Nomenclature and Classification as a mineral species (IMA 2015-003). The mineral was first described on material from the Eleonore Iron mine, Dünsberg, near Giessen, Hesse, Germany, but during this study further samples were required and a neotype locality is the Rotläufchen mine, Waldgirmes, Wetzlar, Hesse, Germany, where eleonorite is associated with goethite, rockbridgeite, dufrénite, kidwellite, variscite, matulaite, planerite, cacoxenite, strengite and wavellite. Usually eleonorite occurs as red-brown prismatic crystals up to 0.2 mm × 0.5 mm × 3.5 mm in size and in random or radial aggregates up to 5 mm across encrusting cavities in massive 'limonite'. The mineral is brittle. Its Mohs hardness is 3. $D_{meas} = 2.92(1)$, $D_{calc} = 2.931$ g cm^{-3}. The IR spectrum is given. Eleonorite is optically biaxial (+), $\alpha = 1.765(4)$, $\beta = 1.780(5)$, $\gamma = 1.812(6)$, $2V_{meas} = 75(10)°$, $2V_{calc} = 70°$. The chemical composition (electron microprobe data, H_2O analysed by chromatography of products of ignition at 1200°C, wt.%) is: Al_2O_3 1.03, Mn_2O_3 0.82, Fe_2O_3 51.34, P_2O_5 31.06, H_2O 16.4, total 99.58. All iron was determined as being trivalent from a Mössbauer analysis. The empirical formula (based on 27 O apfu) is $(Fe_{5.76}^{3+}Al_{0.18}Mn_{0.09}^{3+})_{\Sigma6.03}(PO_4)_{3.92}O(OH)_{4.34} \cdot 5.98H_2O$. The crystal structure ($R = 0.0633$) is similar to that of beraunite and is based on a heteropolyhedral framework formed by $M(1–4)Ø_6$-octahedra (where $M = Fe^{3+}$; $Ø = O^{2-}$, OH^- or H_2O) and isolated PO_4 tetrahedra, with a wide channel occupied by H_2O molecules. Eleonorite is monoclinic, space group $C2/c$, $a = 20.679(10)$, $b = 5.148(2)$, $c = 19.223(9)$ Å, $\beta = 93.574(9)°$, $V = 2042.5(16)$ Å^3 and $Z = 4$. The strongest reflections of the powder X-ray diffraction pattern [d, Å (I,%) (hkl)] are 10.41 (100) (200), 9.67 (38) (002), 7.30 (29) (20$\bar{2}$), 4.816 (31) (111, 004), 3.432 (18) (600, 114, 404, 313), 3.197 (18) (510, 51$\bar{1}$, 006, 31$\bar{4}$, 602), 3.071 (34) (314, 11$\bar{5}$).

* E-mail: nikchukanov@yandex.ru

Introduction

THIS paper concerns the formal validation of eleonorite, known for a long time (Nies, 1877, 1880; Streng, 1881; Palache *et al.*, 1951), but which has had an ambiguous status. The mineral was first described from material from the abandoned Eleonore Iron mine, Dünsberg, near Giessen, Hesse, Germany, and has since been identified in oxidized zones of many other iron deposits where it was considered to be an oxidized variety of beraunite. However there are substantial differences between these two minerals in physical properties and some crystal chemical features. Beraunite was described as a new mineral by Breithaupt (1841). The mineral is typically green, dark blue-green or greenish-grey and is characterized by much lower refractive indices than that of eleonorite. In dark green beraunite from Campanian age marls of Mullica Hill, New Jersey, USA, 83% Fe^{2+} resides in the central $M(1)$ site with mean $M(1)$–O distance 2.11 Å, whereas the other octahedral cation sites $M(2)$, $M(3)$ and $M(4)$ (with mean M–O distances 2.01 to 2.02 Å) are occupied by Fe^{3+} (Moore and Kampf, 1992). In the current International Mineralogical Association (IMA) list of minerals (http://pubsites.uws.edu.au/ima-cmnc/imalist.htm) the formula of beraunite is given as $Fe^{2+}Fe_5^{3+}[PO_4]_4(OH)_5 \cdot 6H_2O$. Unlike beraunite, in eleonorite all octahedral sites are Fe^{3+}-dominant and one of the OH^- groups is substituted by O^{2-}. The mineral and its name were approved by the IMA Commission on New Minerals, Nomenclature and Classification (IMA 2015-003). Specimens of eleonorite (the neotype from the Rotläufchen mine and a specimen from the Gutglück mine) are deposited in the Fersman Mineralogical Museum of the Russian Academy of Sciences, Moscow, Russia, registration numbers 4684/1 and 4684/2, respectively.

Occurrence, general appearance and physical properties

Almost all data given in this paper were obtained for a specimen from the Rotläufchen mine, Waldgirmes, Wetzlar, Hesse, Germany. We consider this material as a neotype specimen of eleonorite and the Rotläufchen mine as a neotype locality of this mineral. Consequently, both Eleonore and Rotläufchen are the type localities of eleonorite. Eleonorite from the Gutglück mine,
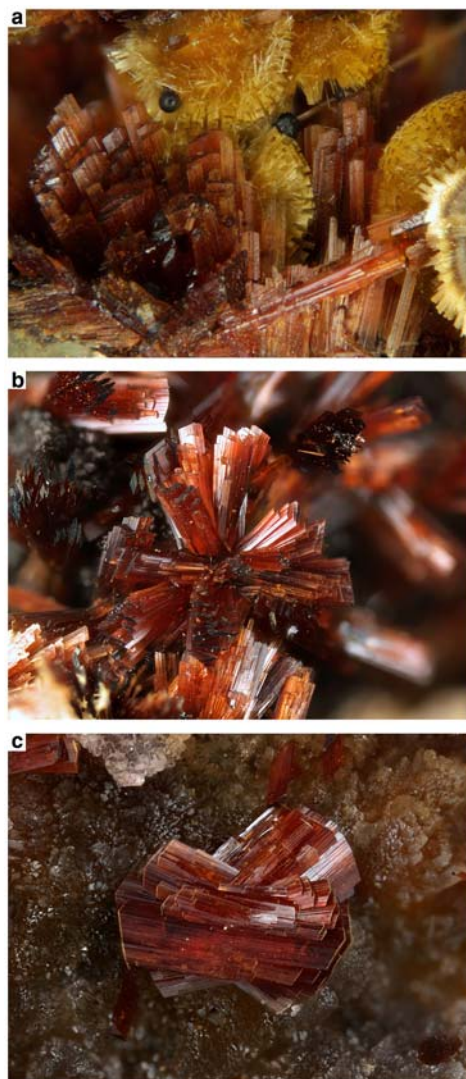

FIG. 1. (*a*) Aggregates of eleonorite with cacoxenite (yellow). Eleonore mine, Giessen. Field of view: 1.0 mm. Photo: Marko Burkhardt; collection: Friedel Pfeiffer. (*b*) Radial aggregates of eleonorite crystals. Gutglück mine, Wetzlar. Field of view: 2.5 mm. Photo: Marko Burkhardt; collection: Friedel Pfeiffer. (*c*) Cluster of split eleonorite crystals on strengite. Rotläufchen mine, Wetzlar. Field of view: 2.3 mm. Photo: Marko Burkhardt; collection: Friedel Pfeiffer.

Braunfels, Wetzlar, Hesse, Germany was also studied by us.

Associated minerals are goethite, quartz, calcite, lepidocrocite, manganese oxides and cacoxenite (Eleonore mine); goethite, rockbridgeite, dufrénite,
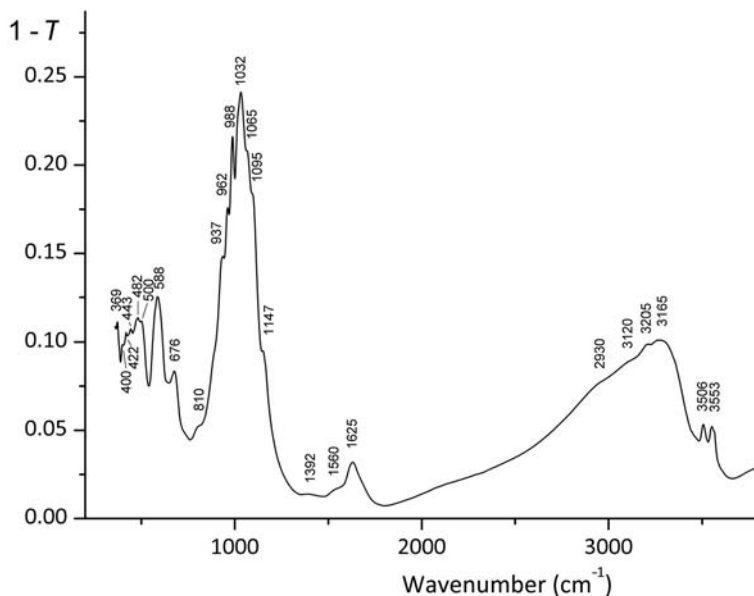
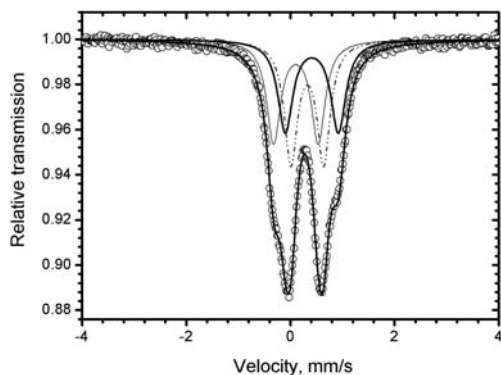FIG. 2. Powder IR absorption spectrum of eleonorite (T = transmittance).

FIG. 3. Mössbauer spectrum of eleonorite.

kidwellite, variscite, matulaite, planerite, cacoxenite, strengite and wavellite (Rotläufchen mine); goethite, quartz, cacoxenite and rockbridgeite (Gutglück mine). In all these localities eleonorite is a supergene mineral formed by the interaction of phosphate-rich solutions that originated from phosphorite deposits with late Devonian iron ores. Most probably, eleonorite is a 'transformational' mineral formed as a result of natural solid-state oxidation of beraunite.

Usually eleonorite forms prismatic crystals (flattened on {100}, or with a rhombic cross section) up to 0.2 mm × 0.5 mm × 3.5 mm in random or radial aggregates up to 5 mm encrusting cavities in massive limonite (Figs 1a–c). More rarely platy crystals are observed. The major crystal forms are {100}, {301} and {30$\bar{1}$}; the subordinate forms are {111} and {1$\bar{1}$1}. Eleonorite crystals are considered as topotactical pseudomorphs after beraunite crystals (see the Discussion section).

Eleonorite is red-brown and has a light red-brown streak, crystals are translucent, with a vitreous lustre.

TABLE 1. Parameters of the Mössbauer spectrum of eleonorite.

Doublet	Isomer shift, mm s^{-1}	Quadrupole splitting, mm s^{-1}	Line width, mm s^{-1}	Relative area, %
1	0.51	1.01	0.34	33.17
2	0.20	0.85	0.32	32.58
3	0.42	0.62	0.30	34.23

TABLE 2. Chemical composition of eleonorite.

Constituent	EDS analyses			WDS analyses			Probe standard
	wt.%*	Range	SD	wt.%**	Range	SD	
Al_2O_3	1.03	0.81–1.36	0.20	0.99	0.84–1.18	0.14	Albite
Mn_2O_3	0.82	0.60–0.97	0.16	0.92	0.83–1.01	0.07	$MnTiO_3$
Fe_2O_3	51.34	50.60–52.08	0.59	52.05	51.37–52.81	0.60	Fe_2O_3
P_2O_5	31.06	30.57–31.49	0.39	33.02	32.64–33.57	0.40	$LaPO_4$
H_2O				16.4(5)			
Total	100.65			103.38			

*Mean of 5 point analyses; **mean of 3 point analyses. According to Mössbauer data, all iron is trivalent. The trivalent state of admixed manganese is assumed taking into account crystal-chemical considerations, as well as oxidizing conditions of formation of the mineral.

EDS – energy-dispersive spectroscopy; WDS – wavelength-dispersive spectoscopy; SD – standard deviation.

TABLE 3. Powder X-ray diffraction data for eleonorite.

I_{obs}	d_{obs}	I_{calc}*	d_{calc}**	hkl
100	10.41	100	10.319	200
38	9.67	39	9.593	002
29	7.30	28	7.255	$20\bar{2}$
1	6.84	1	6.817	202
4	5.162	4	5.160	400
31	4.816	29, 3	4.816, 4.796	111, 004
13	4.424	2, 3, 12	4.458, 4.457, 4.403	$11\bar{2}$, $20\bar{4}$, 112
5	4.085	3	4.122	310
4	4.051	4	4.061	$31\bar{1}$
1	3.976	0.5, 0.5	3.999, 3.966	311, $11\bar{3}$
9	3.737	9	3.737	312
1	3.630	1	3.628	$40\bar{4}$
13	3.481	12	3.486	$11\bar{4}$
18	3.432	11, 4, 3, 9	3.440, 3.434, 3.409, 3.407	600, 114, 404, 313
3	3.304	3	3.304	$60\bar{2}$
18	3.197	6, 2, 11, 4, 5	3.220, 3.202, 3.198, 3.185, 3.176	510, $51\bar{1}$, 006, $31\bar{4}$, 602
11	3.153	10	3.151	511
34	3.071	32, 6	3.070, 3.065	314, $11\bar{5}$
3	2.872	2, 2	2.882, 2.862	$60\bar{4}$, $31\bar{5}$
3	2.821	3	2.822	513
10	2.722	8, 1, 8	2.736, 2.716, 2.712	$51\bar{4}$, 604, $11\bar{6}$
1	2.614	1	2.615	514
9	2.574	5, 4, 1, 3	2.580, 2.574, 2.573, 2.559	800, 020, $31\bar{6}$, 710
1	2.525	2	2.528	$51\bar{5}$
2	2.483	1, 2	2.486, 2.481	022, $22\bar{1}$
3	2.416	3, 1, 2	2.421, 2.410, 2.408	$71\bar{3}$, 515, 222
2	2.331	1, 1, 1	2.334, 2.332, 2.326	$80\bar{4}$, 713, $51\bar{6}$
5	2.306	3, 0.5, 3	2.310, 2.305, 2.303	$71\bar{4}$, 208, 420
1	2.251	1	2.254	$42\bar{2}$

(continued)

TABLE 3. (*contd.*)

I_{obs}	d_{obs}	I_{calc}*	d_{calc}**	hkl
2	2.227	0.5, 2, 1	2.229, 2.228, 2.226	$22\overline{4}$, $40\overline{8}$, 422
1	2.146	1	2.148	423
6	2.105	8, 1	2.107, 2.099	$31\overline{8}$, $42\overline{4}$
4	2.063	2, 2	2.071, 2.064	$91\overline{2}$, 10.0.0
2	2.048	2	2.054	424
2	2.036	1	2.039	517
6	2.000	2, 5	2.005, 2.000	026, 622
2	1.976	1	1.983	$62\overline{3}$
2	1.967	1	1.970	$51\overline{8}$
6	1.919	1, 7, 2	1.923, 1.920, 1.919	$31\overline{9}$, $62\overline{4}$, 0.0.10
2	1.885	2, 0.5	1.881, 1.880	914, 518
2	1.864	3	1.865	319
1	1.821	2	1.822	820
2	1.793	2	1.796	915
1	1.780	2	1.782	1.1.10
1	1.746	1, 2	1.746, 1.743	11.1.1, $22\overline{8}$
2	1.719	2	1.722	$6.0.\overline{10}$
2	1.708	1, 0.5	1.712, 1.704	$91\overline{7}$, 718
2	1.686	2, 1, 1	1.687, 1.687, 1.683	$11.1\overline{4}$, 11.0.6, $71\overline{9}$
1	1.656	0.5, 0.5, 1	1.654, 1.654, 1.652	$1.1.\overline{11}$, $13\overline{3}$, $12.0.\overline{4}$
6	1.614	0.5, 2, 7	1.617, 1.613, 1.610	$33\overline{3}$, $13\overline{4}$, 10.2.0
2	1.602	2	1.599	$0.0.\overline{12}$
1	1.579	0.5, 0.5	1.576, 1.576	$7.1.\overline{10}$, 10.2.2
3	1.569	2, 1	1.566, 1.565	334, $13\overline{5}$
5	1.537	4, 3	1.535, 1.533	628, $2.2.\overline{10}$
1	1.520	0.5	1.519	335
2	1.498	1, 0.5, 0.5	1.496, 1.495, 1.494	8.0.10, $4.2.\overline{10}$, 534
1	1.476	1	1.474	14.0.0
3	1.458	1, 2	1.457, 1.454	$9.1.\overline{10}$, 4.2.10
1	1.444	1, 1	1.447, 1.441	137, $12.0.\overline{8}$
2	1.434	0.5, 0.5, 0.5	1.435, 1.434, 1.433	$14.0.\overline{4}$, $53\overline{6}$, $33\overline{7}$
2	1.426	1, 2	1.425, 1.422	$12.2.\overline{2}$, 13.1.4
1	1.409	0.5, 0.5	1.411, 1.406	10.2.6, $3.1.\overline{13}$
1	1.376	0.5, 0.5	1.377, 1.374	$33\overline{8}$, $93\overline{1}$
1	1.333	0.5	1.329	15.1.0
2	1.323	2	1.322	$12.0.\overline{10}$
1	1.308	0.5	1.307	$9.1.\overline{12}$

*For the calculated pattern, only reflections with intensities ≥ 0.5 are given. **For the unit cell parameters calculated from single-crystal data.

The mineral is brittle, with Mohs hardness of 3. Cleavage is perfect on (100). Density measured by flotation in heavy liquids (mixtures of diiodmethane and ethanol) is 2.92(1) g cm^{-3}. Density calculated using the empirical formula is 2.931 g cm^{-3}.

Eleonorite is optically biaxial (+), $\alpha = 1.765(4)$, $\beta = 1.780(5)$, $\gamma = 1.812(6)$, $2V_{meas} = 75(10)°$, $2V_{calc.} = 70°$. Dispersion of optical axes is very strong, $r > v$. The orientation is $X = b$; the X and Z axes lie in the (100) plane at an angle close to 90° with one another. Pleochroism is strong; Z (brown-red) $\gg Y \geq X$ (brownish yellow).

Infrared spectroscopy

In order to obtain an infrared (IR) absorption spectrum, a powdered sample of eleonorite was

TABLE 4. Crystal parameters, data collection and structure refinement
details for the crystal of eleonorite.

Crystal data	
Formula	$Fe_6^{3+}(PO_4)_4O(OH)_4 \cdot 6H_2O$
Formula weight (g)	907.1
Temperature (K)	293
Cell setting	Monoclinic
Space group	$C2/c$
a (Å)	20.68(1)
b (Å)	5.148(2)
c (Å)	19.22(1)
β (°)	93.57(1)
V (Å^3)	2042(2)
Z	4
Crystal size (mm)	0.13 x 0.15 x 0.18
Crystal form	Anhedral grain
Data collection	
Diffractometer	SMART APEX2 CCD
Radiation; λ	Mo$K\alpha$; 0.71073
Absorption coefficient, μ (mm^{-1})	4.596
$F(000)$	1788
Data range θ (°); h, k, l	1.97–31.05; $-29 < h < 29$, $-7 < k < 7, -27 < l < 27$
No. of measured reflections	12,947
Total reflections (N_2)/unique(N_1)	3141/2230
Criterion for observed reflections	$I > 2\sigma(I)$
R_{int} (%)	7.44
Refinement	
Refinement on	Full-matrix least squares on F
Weighting scheme	$1/(\sigma^2(F) + 0.0025F^2)$
R_1, wR_2*	6.08, 8.60
Goof	0.99
Max./min. residual e density, (e Å^{-3})	1.02/–0.82

*$R_1 = \sum ||F_{obs}| - |F_{calc}|| / \sum |F_{obs}|$; $wR_2 = \{\sum[w(F_{obs}^2 - F_{calc}^2)^2] / \sum[w(F_{obs}^2)^2]\}^{1/2}$;
Goof $= \{\sum[w(F_{obs}^2 - F_{calc}^2)] / (n - p)\}^{1/2}$ where n is a number of reflections
and p is the number of refined parameters.

mixed with dried KBr, pelletized, and analysed
using an ALPHA FTIR spectrometer (Bruker
Optics) with a resolution of 4 cm^{-1} and 16 scans
(Fig. 2). The IR spectrum of an analogous pellet of
pure KBr was used as a reference. Absorption
bands in the IR spectrum and their assignments are
(ν (cm^{-1}); s – strong band, sh – shoulder) 3553,
3506, 3265s, 3205, 3120sh, 2930sh (O–H stretching
vibrations of OH$^-$ anions and H$_2$O molecules), 1625,
1560sh (bending vibrations of H$_2$O molecules),
1147, 1095sh, 1065sh, 1032s, 988s [ν$_3(F_2)$ –
antisymmetric P–O stretching vibrations of PO$_4^{3-}$
anions], 962s, 937s [ν$_1(A_1)$ – symmetric P–O
stretching vibrations of PO$_4^{3-}$ anions], 810sh, 676

(Fe^{3+}···O–H bending vibrations), 588s [triply
degenerate ν$_4(F_2)$ O–P–O bending mode of PO$_4^{3-}$
anions]. The weak absorption at 1392 cm^{-1} is
possibly a combination band. Low frequency
bands at 500, 482, 443, 422 and 369 cm^{-1}
correspond to lattice modes involving Fe^{3+}–O
stretching and ν$_2(E)$ O–P–O bending vibrations,
possibly combined with libration modes of H$_2$O
molecules. Exact assignment of these bands is
ambiguous. The presence of the nondegenerate
ν$_1(A_1)$ bands of symmetric P–O stretching vibrations
in PO$_4^{3-}$ anions and the splitting of the degenerate
ν$_3(F_2)$ band of the antisymmetric stretching modes
of PO$_4^{3-}$ anions reflect the distortion of the PO$_4$

TABLE 5. Fractional coordinates, site multiplicities (Q) and equivalent displacement parameters of atoms (U_{eq}, Å^2) in the structure of eleonorite.*

Site	x/a	y/b	z/c	Q	$U_{eq/iso}$**
$M1$	0	0	0	4	0.0128(3)
$M2$	0.25	0.25	0	4	0.0147(3)
$M3$	0.0438(1)	0.2696(2)	0.17236(4)	8	0.0106(2)
$M4$	0.1074(1)	0.0318(2)	0.41238(4)	8	0.0110(2)
P1	0.1048(1)	0.4782(3)	0.02621(8)	8	0.0082(4)
P2	0.4073(1)	0.0388(3)	0.18234(8)	8	0.0088(4)
O1	0.1774(2)	0.4854(8)	0.0152(2)	8	0.013(1)
O2	0.4283(2)	0.2443(7)	0.0180(2)	8	0.013(1)
O3	0.4242(2)	0.2417(7)	0.4991(2)	8	0.016(1)
O4	0.0927(2)	0.438(1)	0.1022(2)	8	0.021(1)
O5	0.4790(2)	0.046(1)	0.1686(2)	8	0.015(1)
O6	0.1016(2)	0.477(1)	0.2412(2)	8	0.017(1)
O7	0.3782(2)	0.308(1)	0.1652(2)	8	0.012(1)
O8	0.1302(2)	0.341(1)	0.3645(2)	8	0.014(1)
OH1	0.0074(2)	0.046(1)	0.3965(2)	8	0.015(1)
OH2	0.1919(2)	0.018(1)	0.4629(2)	8	0.013(1)
H1$_{OH2}$	0.214(3)	−0.03(1)	0.424(3)	8	0.019*
OH3	0	0.100(1)	0.25	4	0.015(2)
H2$_{OH3}$	0	−0.081(6)	0.25	4	0.036*
$W1$	0.3853(2)	0.473(1)	0.3217(3)	8	0.022(1)
H3$_{W1}$	0.400(4)	0.37(1)	0.360(3)	8	0.040*
H4$_{W1}$	0.392(4)	0.38(1)	0.281(2)	8	0.040*
$W2$	0.2467(2)	0.086(1)	0.0974(2)	8	0.016(1)
H5$_{W2}$	0.240(3)	0.22(1)	0.130(3)	8	0.028*
H6$_{W2}$	0.284(3)	−0.01(1)	0.113(4)	8	0.028*
$W3$	0.2315(3)	0.355(1)	0.2149(3)	8	0.038(2)
H7$_{W3}$	0.187(2)	0.38(2)	0.210(4)	8	0.046*
H8$_{W3}$	0.244(2)	0.34(2)	0.263(2)	8	0.046*

*$M1–4$ = Fe^{3+}; OH1 = $O_{0.5}(OH)_{0.5}$; OH2–3 = OH; $W1–3$ = H_2O. **U_{eq} is defined as one third of the trace of the orthogonalized U^{ij} tensor.

tetrahedra and lowering of their symmetry. Two $v_1(A_1)$ bands (at 937 and 962 cm^{-1}) correspond to two structurally nonequivalent PO_4^{3-} groups, which is in agreement with structural data. The IR spectrum of eleonorite resembles that of beraunite (Chukanov, 2014; see Table 10). The main differences are observed in the regions of O–H stretching, Fe···O–H bending and Fe–O stretching vibrations.

Mössbauer spectroscopy

The ^{57}Fe Mössbauer spectrum (Fig. 3, Table 1) was collected in a constant acceleration transmission mode, in the velocity range ±4 mm s^{-1}, with a 10 mCi ^{57}Co/Rh source, at 298 K. Data were stored in a 1024 channel MCS memory unit and were fitted using Lorentzian line shapes with a least-squares fitting procedure using the *NORMOS* program. Isomer shifts were calculated relative to α-Fe. The Mössbauer spectrum of eleonorite is a superposition of three doublets due to octahedrally coordinated trivalent iron. Taking into account site multiplicities and the fact that the ratio of relative areas of the doublets is very close to 1:1:1, one can assume that the doublets are due to Fe^{3+} at the $M1+M2$, $M3$ and $M4$ sites (see description of the crystal structure below).

Chemical data

Chemical electron microprobe analyses were carried out using an Oxford INCA Wave 700

TABLE 6. Anisotropic atomic displacement parameters for eleonorite ($Å^2$).

Site	U^{11}	U^{22}	U^{33}	U^{12}	U^{13}	U^{23}
M1	0.0125(6)	0.0086(5)	0.0172(6)	−0.0007(4)	0.0010(4)	0.0029(4)
M2	0.0165(6)	0.0124(5)	0.0150(6)	0.0009(5)	−0.0001(5)	−0.0001(5)
M3	0.0158(4)	0.0083(4)	0.0078(4)	−0.0013(3)	0.0015(3)	−0.0011(3)
M4	0.0149(4)	0.0074(4)	0.0107(4)	−0.0002(3)	0.0019(3)	0.0008(3)
P1	0.0126(6)	0.0058(6)	0.0063(6)	−0.0002(5)	0.0000(5)	0.0003(5)
P2	0.0124(6)	0.0070(6)	0.0068(6)	0.0000(5)	−0.0019(5)	0.0006(5)
O1	0.012(2)	0.011(2)	0.017(2)	0.005(2)	0.001(2)	0.001(2)
O2	0.016(2)	0.010(2)	0.013(2)	−0.004(2)	−0.002(2)	−0.001(2)
O3	0.018(2)	0.007(2)	0.022(2)	−0.002(2)	0.002(2)	0.002(2)
O4	0.027(2)	0.027(2)	0.009(2)	−0.008(2)	0.001(2)	−0.001(2)
O5	0.014(2)	0.015(2)	0.016(2)	0.002(2)	−0.001(2)	0.007(2)
O6	0.020(2)	0.020(2)	0.009(2)	−0.004(2)	0.001(2)	−0.003(2)
O7	0.014(2)	0.005(2)	0.018(2)	0.001(2)	0.001(2)	0.000(2)
O8	0.017(2)	0.010(2)	0.014(2)	0.002(2)	−0.001(2)	0.006(2)
OH1	0.013(2)	0.025(2)	0.006(2)	0.006(2)	0.000(2)	0.006(2)
OH2	0.013(2)	0.011(2)	0.013(2)	0.004(2)	−0.002(2)	0.001(2)
OH3	0.024(3)	0.008(2)	0.013(3)	0	0.005(2)	0
W1	0.026(2)	0.012(2)	0.027(3)	−0.006(2)	0.002(2)	−0.006(2)
W2	0.019(2)	0.017(2)	0.013(2)	0.003(2)	0.002(2)	0.003(2)
W3	0.031(3)	0.043(3)	0.038(3)	0.006(3)	−0.002(2)	−0.016(3)

electron microprobe (WDS mode, 20 kV, 20 nA, 300 μm beam diameter) and a VEGA TS 5130MM SEM equipped with EDX analyser (INCA Si(Li) detector, at an operating voltage of 20 kV and a beam current of 0.6 nA, beam rastered on an area 8 μm × 8 μm). The contents of other elements with $Z > 8$ are below detection limits. The H_2O content was analysed by chromatography of products of ignition at 1200°C. Analytical data are given in Table 2. The empirical formulae (based on 27 O apfu) are $(Fe^{3+}_{5.68}Al_{0.17}Mn^{3+}_{0.10})_{\Sigma6.03}P_{4.055}$ $H_{15.87}O_{27}$ (calculated from the WDS analyses) and $(Fe^{3+}_{5.76}Al_{0.18}Mn^{3+}_{0.09})_{\Sigma6.03}P_{3.92}H_{16.30}O_{27}$ (calculated from the EDS analyses). Taking into account structural data (see description of the crystal structure below) these formulae can be rewritten as $(Fe^{3+}_{5.68}Al_{0.17}Mn^{3+}_{0.10})_{\Sigma5.95}(PO_4)_{4.055}O$ $(OH)_{3.69}·6.09H_2O$ and $(Fe^{3+}_{5.76}Al_{0.18}Mn^{3+}_{0.09})_{\Sigma6.03}$ $(PO_4)_{3.92}O(OH)_{4.34}·5.98H_2O$. The idealized end-member formula is $Fe^{3+}_6(PO_4)_4O(OH)_4·6H_2O$, which requires Fe_2O_3 52.82, P_2O_5 31.29, H_2O 15.89, total 100.00 wt.%.

The Gladstone-Dale compatibility index is: $1 − (K_p/K_c) = 0.033$ ('excellent'). Eleonorite dissolves slowly in dilute hydrochloric acid without producing any gases. Tests with potassium ferrocyanide and potassium ferricyanide show the presence of Fe^{3+} and the absence of Fe^{2+}.

X-ray diffraction data and crystal structure

Powder X-ray diffraction data were collected with a Rigaku R-AXIS Rapid II single-crystal diffractometer equipped with a cylindrical image plate detector using Debye-Sherrer geometry ($d = 127.4$ mm). Data (in Å for Co$K\alpha$) are given in Table 3. The unit-cell parameters refined from the powder data are $a = 20.694(6)$, $b = 5.143(1)$, $c = 19.236(7)$ Å, $\beta = 93.52(2)°$, $V = 2044(2)$ Å^3.

A red grain (0.13 mm × 0.15 mm × 0.18 mm) was used for single-crystal X-ray data collection. Data were collected at room temperature on a SMART APEX2 diffractometer (Bruker, 2009) with graphite-monochromatized Mo$K\alpha$ radiation ($\lambda = 0.71073$ Å) and a CCD detector using the ω−θ scanning mode. Raw data were integrated by using the program *SAINT* and then scaled, merged, and corrected for Lorentz and polarization effects using the *SADABS* package. A total of 12,947 reflections within the sphere limited by $\theta = 31.05°$ was measured. Experimental details of the data collection and refinement results are listed in Table 4. The structure determination and refinement were carried out using the *JANA2006* program package (Petříček *et al.*, 2006). Illustrations were produced with the *JANA2006* program package in combination with

TABLE 7. Selected interatomic distances and O–P–O angles in eleonorite.*

Bond		Bond length, Å	Bond		Bond length, Å
$M1$	–OH1	2.019(4) × 2	P1	–O4	1.511(5)
	–O2	2.028(5) × 2		–O1	1.531(5)
	–O3	2.055(4) × 2		–O3	1.549(4)
	$<M1–O>$	2.034		–O2	1.559(5)
	$\Delta^{(M1)}/\lambda_{oct}^{(M1)}$	2.34 / 1.03		$<P1–O>$	1.538
$M2$	–OH2	1.938(6) × 2	P2	–O5	1.523(5)
	–O1	1.965(5) × 2		–O6	1.526(5)
	–$W2$	2.059(4) × 2		–O7	1.536(6)
	$<M2–O>$	1.987/1.003		–O8	1.538(4)
	$\Delta^{(M2)}/\lambda_{oct}^{(M2)}$	27.23		$<P2–O>$	1.531
$M3$	–O4	1.940(8)			
	–O5	1.952(4)	Angle		Angle value, °
	–OH3	1.995(7)	O4–P1–O1		111.1(2)
	–OH1	2.008(8)	O4–P1–O3		109.8(2)
	–O6	2.030(8)	O4–P1–O2		109.5(2)
	–$W1$	2.113(4)	O1–P1–O3		107.4(2)
	$<M3–O>$	2.007	O1–P1–O2		110.1(2)
	$\Delta^{(M3)}/\lambda_{oct}^{(M3)}$	32.73/1.003	O3–P1–O2		108.9(2)
$M4$	–O8	1.913(5)	O5–P2–O6		110.4(2)
	–O7	1.921(4)	O5–P2–O7		108.3(2)
	–OH2	1.945(9)	O5–P2–O8		112.0(2)
	–OH1	2.073(5)	O6–P2–O7		109.0(2)
	–O2	2.156(6)	O6–P2–O8		109.9(2)
	–O3	2.196(6)	O7–P2–O8		107.1(2)
	$<M4–O>$	2.034			
	$\Delta^{(M4)}/\lambda_{oct}^{(M4)}$	129.22/1.029			

*Octahedral distortion (Δ) and quadratic elongation (λ_{oct}) are calculated as $\Delta = (1/6)\sum_{i=1-6}\{[(M–O)_i - <M–O>]/<M–O>\}^2 \times 10^4$ (Brown and Shannon, 1973) and $\lambda_{oct} = (1/6)\sum_{i=1-6}(l_i/l_o)^2$ (Robinson *et al.*, 1971).

TABLE 8. Geometrical characteristics of hydrogen bonds in the structure of eleonorite.

$D–H\cdots A$	$D–H$, Å	φ (H–D–H), °	$H\cdots A$, Å	$A–A$, Å	φ ($A\cdots H\cdots A$), °	$D–A$, Å	φ ($D–H\cdots A$), °
OH2–H1$\cdots W2$	0.94(6)	—	2.18(7)	2.76(1)	77(4)	2.81(1)	127(5)
OH2–H1$\cdots$O1			2.47(6)			2.72(1)	95(4)
OH3–H2$\cdots$O5	0.93(3)	—	2.50(2)	3.195(9)	79.5(1)	2.80(1)	140.3(1)
OH3–H2$\cdots$O5			2.50(2)			2.80(1)	140.3(1)
$W1$–H3$\cdots$O4	0.94(6)	108(4)	2.36(7)	2.895(6)	103(3)	2.83(1)	141(5)
$W1$–H3$\cdots$OH1			2.45(8)			2.85(1)	106(5)
$W1$–H4$\cdots$O6	0.94(5)		2.12(7)	2.495(6)	69(1)	2.85(1)	133(5)
$W1$–H4$\cdots$O7			2.26(4)			3.12(1)	153(3)
$W2$–H5$\cdots W3$	0.95(6)	109(5)	1.79(6)			2.68(1)	155(5)
$W2$–H6$\cdots$O8	0.95(6)		1.96(6)			2.89(1)	169(6)
$W3$–H7$\cdots$O6	0.94(4)	109(5)	1.96(5)			2.84(1)	155(3)
$W3$–H8$\cdots W3$	0.94(4)		2.6(1)			2.98(1)	106(4)

TABLE 9. Bond valence calculations for eleonorite.*

Site	$M1$	$M2$	$M3$	$M4$	P1	P2	H1	H2	H3	H4	H5	H6	H7	H8	V_i
O1		$0.57^{\rightarrow}$ $0.57^{\times2\downarrow}$			1.26		0.08								1.91
O2	$0.48^{\rightarrow}$ $0.48^{\times2\downarrow}$			0.34	1.17										1.99
O3	$0.45^{\rightarrow}$ $0.45^{\times2\downarrow}$			0.31	1.20										1.96
O4			0.61		1.33				0.10						2.04
O5			0.59			1.29		$0.08^{\rightarrow}$ $0.08^{\times2\downarrow}$							1.96
O6			0.48			1.28				0.14			0.19		2.09
O7				0.64		1.24				0.12					2.06
O8				0.66		1.24						0.19			2.09
OH1[a]	$0.50^{\rightarrow}$ $0.50^{\times2\downarrow}$		0.51	0.43					0.08						1.52
OH2		$0.62^{\rightarrow}$ $0.62^{\times2\downarrow}$		0.60				0.90							2.12
OH3			$0.53^{\times2\rightarrow}$ $0.53^{\downarrow}$						0.91						1.97
$W1$			0.38								0.90	0.90			2.18
$W2$		$0.44^{\rightarrow}$ $0.44^{\times2\downarrow}$						0.13			0.85	0.86			2.28
$W3$[b]											0.27		0.90	0.87+ 0.07	2.11
V_i	2.86	3.26	3.1	2.98	4.96	5.05	1.03	1.07	1.08	1.16	1.12	1.05	1.09	0.94	

*BVS for hydrogen bonds was calculated using $Ro = 0.907$ and $B = 0.28$ for O–H and $Ro = 0.990$ and $B = 0.59$ for O···H (Brown, 2002). [a]$O_{0.5}(OH)_{0.5}$. Hydrogen atom contribution is omitted in the BVS. [b]Water molecule that does not have short contacts with cations.
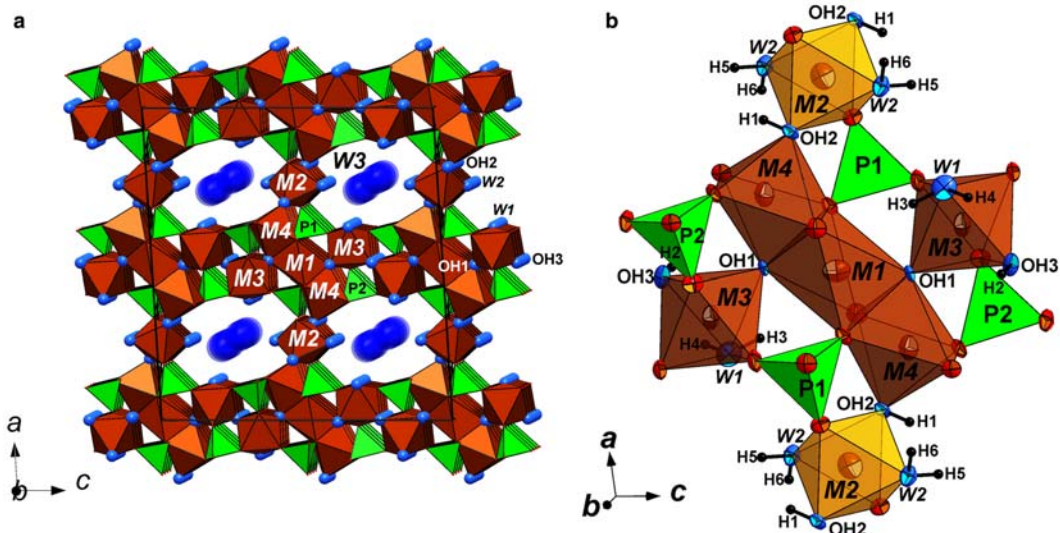
FIG. 4. General view of the crystal structure of eleonorite without indication of the hydrogen atoms (*a*; the unit cell is outlined) and *h* cluster (*b*). *M*2-octahedra (light brown colour) belong to two adjacent *h* clusters.

the program *DIAMOND* (Brandenburg, 1999). In accordance with the analysis of systematic absence of reflections, space group $C2/c$ (the usual space group for minerals with the beraunite-type structure) was chosen. Atom scattering factors for neutral atoms together with anomalous dispersion corrections were taken from *International Tables for X-Ray Crystallography* (Ibers and Hamilton, 1974). The initial model (except for hydrogen atoms) for the eleonorite structure refinement was based on the atom coordinates of the beraunite structure (Moore and Kampf, 1992). Eight atom positions were found in difference-Fourier maps and were inserted into the refinement with soft restraints of 0.95(3) Å on the O–H distances. It was accepted that isotropic displacement parameters U_{iso} of each H atom is 1.5 times greater than equivalent atomic displacement parameter U_{eq} of the corresponding donor O atom. The final refinement cycles converged with $R_1 = 6.08$, $wR_2 = 8.60$, Goof = 0.99 for 2230 reflections with $I > 2\sigma(I)$. The highest peak and the deepest hole in the final residual electron density map were 1.02 and $-0.82\ e\ \text{Å}^{-3}$, respectively. Table 5 lists the fractional atom coordinates, occupancy, site symmetry and equivalent/isotropic atomic displacement parameters. Anisotropic atomic displacement parameters (U^{ij}) are presented in Table 6. Selected interatomic distances and angles in the PO_4 tetrahedra are given in Table 7. Geometrical characteristics of hydrogen bonds are presented in Table 8.

Bond-valence sum (BVS) calculations can be used for the indirect verification of mixed oxygen/hydroxyl site presence in the structure. Bond-valence sum calculations (Table 9) were performed using bond-length parameters for Fe^{3+}–O, P^{5+}–O (Brown and Altermatt, 1985) and H^{+}–O (Brown, 2002). The value of BVS for the OH1-site (1.52 vu) confirms the mixed site occupancy by OH^- and O^{2-}.

Discussion

Eleonorite was first observed by August Nies (1877) in the Eleonore Iron mine as small red-brown tabular crystals overgrown by cacoxenite. Three years later he described it as a new species, a basic phosphate of Fe^{3+} (Nies, 1880). Streng (1881) reported another occurrence of eleonorite, the Rotläufchen (Rothläufchen) mine, and described it as an iron phosphate with the stoichiometry $Fe:P:H_2O = 3:2:4$, which corresponds to the present day idealized formula of the mineral. However the axial ratios for monoclinic eleonorite were erroneously determined by A. Streng as $a:b:c = 2.755:1:4.0157$, $\beta = 48°33'$. Frondel (1949) published new chemical analyses of beraunite, and showed that in samples from Middletown, New Jersey, USA, iron is partly bivalent. From these data, it was assumed that Fe^{2+} and Fe^{3+} may occupy different sites in the crystal structure of beraunite. Subsequent structural studies confirmed this assumption. Based on structural and

TABLE 10. Comparative data for eleonorite and closely related minerals.*

Mineral	Eleonorite	Beraunite	Mn-rich beraunite-type mineral
Simplified formula	$F_6^{3+}(PO_4)_4O(OH)_4 \cdot 6H_2O$	$Fe^{2+}F_5^{3+}(PO_4)_4(OH)_5 \cdot 6H_2O$	$F_{5.5}^{3+}Mn_{0.5}^{2+}(PO_4)_4(OH)_6 \cdot 5H_2O$
Crystal system, space group	Monoclinic, $C2/c$	Monoclinic, $C2/c$	Monoclinic, $C2/c$
a, Å	20.679	20.630–20.953	20.760(3)
b, Å	5.148	5.164–5.171	5.154(1)
c, Å	19.223	19.22–19.266	19.248(2)
β, °	93.574	93.30–93.61	93.55(1)
V, Å^3	2042.5	2044–2084	2055.4(3)
Z	4	4	4
Strong lines of the powder X-ray diffraction pattern: d, Å (I, %)	10.41 (100) 9.67 (38) 7.30 (20) 4.816 (31) 3.432 (18) 3.197 (18) 3.071 (34)	10.295 (100) 7.250 (17) 5.147 (12) 3.438 (29) 3.298 (15) 3.150 (16) 2.575 (15)	10.39 (100) 9.62 (50) 7.28 (50) 4.82 (60) 4.44 (50) 3.208 (40) 3.080 (60)
Optical data	Biaxial (+) $\alpha = 1.765$ $\beta = 1.780$ $\gamma = 1.812$ $2V = 75°$	Biaxial (+) or (–) $\alpha = 1.69–1.707$ $\beta = 1.73–1.735$ $\gamma = 1.73–1.738$ $2V = 20°$ (for an optically negative sample)	Biaxial (+) $\alpha = 1.768$ $\beta = 1.774$ $\gamma = 1.783$ $2V = 78°$
Strong and characteristic bands in the IR spectrum	3553, 3506, 3265, 1032, 988, 588, 500, 482	3565, 3490, 3370, 1033, 990, 866, 608, 454	No data reported
Density (g cm^{-3})	2.92 (meas.) 2.931 (calc.)	2.894 (calc.)	2.99 (meas.) 2.978 (calc.)
References	This work	Blanchard and Denahan (1968), Moore and Kampf (1992), Sejkora *et al.* (2006), Chukanov (2014)	Marzoni Fecia di Cossato *et al.* (1989)

*The reflections of the powder X-ray diffraction pattern of beraunite are given for a Zn- and Al-rich variety (Sejkora *et al.*, 2006).

TABLE 11. Crystal data for phosphate and phosphate-sulfate minerals with only Fe^{3+} as a species-defining metal cation.

Chemical formula / Mineral	Space grp. Z	Unit-cell parameters			References
		a, Å / α, °	b, Å / β, °	c, Å / γ, °	
$Fe^{3+}(PO_4)$ Heterosite	$Pmnb$ 4	5.83	9.76	4.769	Eventoff et al. (1972)
$Fe^{3+}(PO_4)$ Rodolicoite	$P3_12$ 3	5.036	5.036	11.255 120	Cipriani et al. (1997); Arnold (1986)
$Fe_3^{3+}O_3(PO_4)$ Grattarolaite	$R3m$ 3	8.006	8.006	6.863 120	Cipriani et al. (1997), Modaressi et al. (1983)
$(Fe^{3+},Mn^{2+})_3(PO_4)_2(OH,H_2O)_3$ Kryzhanovskite	$Pbna$ 4	9.518	9.749	8.031	Moore and Araki (1976)
$Fe^{3+}(PO_4) \cdot 2H_2O$ Strengite	$Pbca$ 8	8.722	9.878	10.119	Taxer and Bartl (2004)
$Fe^{3+}(PO_4) \cdot 2H_2O$ Phosphosiderite	$P2_1/n$ 4	5.3	9.77 90.6	8.73	Moore (1966)
$Fe^{3+}(PO_4) \cdot 3H_2O$ Koninckite	n.d.	11.95– 11.977	11.95– 11.977	14.52– 14.625	Sakurai et al. (1987)
$Fe_3^{3+}(PO_4)_2(OH)_3 \cdot 5H_2O$ Ferristrunzite	$P\bar{1}$ or $P1$ 2	10.01 90.50	9.73 96.99	7.334 116.43	Peacor et al. (1987)
$Fe_3^{3+}(PO_4)_2(OH)_3 \cdot 5H_2O$ Allanpringite	$P2_1/n$ 4	9.777	7.358 92.19	17.380	Kolitsch et al. (2006)
$Fe_3^{3+}(PO_4)_2(OH)_3 \cdot 5H_2O$ Santabarbaraite	X-ray amorphous				Pratesi et al. (2003)
$Fe_6^{3+}(PO_4)_4O(OH)_4 \cdot 5H_2O$ Eleonorite	$C2/c$ 4	20.68	5.148 93.574	19.22	This work
$Fe_{5.3}^{3+}(PO_4)_4(OH)_4 \cdot 6.7H_2O$ Tinticite	$P\bar{1}$ 1	7.965 103.94	9.999 115.91	7.644 67.86	Rius et al. (2000)
$Fe_2^{3+}[PO_3(OH)]_2(SO_4) \cdot 5–6H_2O$ Camaronesite	$R32$ 9	9.083	9.083	42.944 120	Kampf et al. (2013)
$Fe_2^{3+}(PO_4)(SO_4)(OH) \cdot 6H_2O$ Destinezite	$P\bar{1}$ 2	9.570 98.74	9.716 107.90	7.313 63.86	Peacor et al. (1999)
$Fe_2^{3+}(PO_4)(SO_4)(OH) \cdot 6H_2O$ Diadochite	X-ray amorphous				Peacor et al. (1999)

compositional data, Moore and Kampf (1992) suggested the end-member formulae for beraunite-type minerals $Fe^{2+}Fe_5^{3+}(OH)_5(H_2O)_4(PO_4)_4 \cdot 2H_2O$ and $Fe_6^{3+}O(OH)_4(H_2O)_4(PO_4)_4 \cdot 2H_2O$. The latter formula corresponds to that of eleonorite. Different varieties of beraunite with intermediate values of the $Fe^{2+}:Fe^{3+}$ ratio are known (Fanfani and Zanazzi, 1967), thus, the existence of the continuous solid-solution series between beraunite and eleonorite is not excluded.

The crystal structure of eleonorite is similar to that of beraunite and is based on heteropolyhedral framework formed by $M(1–4)\emptyset_6$-octahedra (where $M = Fe^{3+}$; $\emptyset = O^{2-}$, OH^- or H_2O) and isolated PO_4 tetrahedra (Fig. 4), with a wide channel occupied by H_2O molecules. In accordance with Moore (1969, 1970) and Moore and Kampf (1992) the structures of basic iron phosphates are formed by the condensation of so-called 'h clusters'. The general formula of the isolated h cluster in the beraunite-type structures is $M1 (M2)_{1/2}(M3)_2(M4)_2[(OH)_5(H_2O)_4](PO_4)_4$ (Fig. 4b). Along a, the h clusters are linked via common $M2$ octahedra, whereas in other directions the clusters link via the oxygen atoms of PO_4 tetrahedra and OH3 groups. In beraunite-type structures, the h cluster contains a trimer of face-shared $M1$ and $M4$ octahedra (the $M1$–$M4$ distance is 2.875(1) Å), where the inner $M1O_4(OH1)_2$ octahedron occupies the $4a$ site and

outer $M4O_4(OH1)(OH2)$ octahedra occupy $8f$ sites. In the structure of eleonorite all the sites are occupied by Fe^{3+}, whereas in beraunite $M1$ is occupied predominantly by Fe^{2+}. This leads to the shortening of the average $M1$–Ø distance from 2.110 Å in beraunite (Moore and Kampf, 1992) to 2.034 Å in eleonorite. This is in a good agreement with ionic radii of Fe^{2+} and Fe^{3+}, 0.61 and 0.55 Å, respectively (Shannon, 1976). The trimer of face-shared octahedra is connected to $M3O_3Ø_3$ octahedra via the OH1 group. The $W3$ site in the wide channels of the eleonorite structure is occupied by H_2O molecules linked to each other and to PO_4^{3-} groups by hydrogen bonds (Table 8). Along with eleonorite $Fe_6^{3+}(PO_4)_4O$ $(OH)_4{\cdot}6H_2O$ and beraunite $Fe^{2+}Fe_5^{3+}(PO_4)_4(OH)_5{\cdot}$ $6H_2O$, the beraunite group includes an insufficiently studied beraunite-type mineral with $Mn^{2+}{:}Fe^{3+} =$ 0.52:5.48, possibly, the Mn^{2+} analogue of beraunite (Marzoni Fecia di Cossato *et al.*, 1989) and recently discovered tvrdýite $Fe^{2+}Fe_2^{3+}Al_3(PO_4)_4(OH)_5{\cdot}6H_2O$ (Sejkora *et al.*, 2015; Sejkora *et al.*, 2016). From the comparative data for eleonorite, beraunite and the abovementioned Mn-rich beraunite-type mineral given in Table 10, it is clear that eleonorite differs substantially from beraunite in optical characteristics.

In Nature numerous transformational series are known which are the result of the oxidation of Fe^{2+} to Fe^{3+} with coupled substitution of OH^- for O^{2-} and/or H_2O for OH^- (in some cases, leaching of alkaline cations takes place as well). Among phosphate minerals, the well-known transformation series of this kind are vivianite $Fe^{2+}Fe_2^{2+}$ $(PO_4)_2{\cdot}8H_2O$ → metavivianite $Fe^{2+}Fe_2^{3+}(PO_4)_2$ $(OH)_2{\cdot}6H_2O$ → Fe^{3+}-analogue of metavivianite $(Fe^{3+},Fe^{2+})Fe_2^{3+}(PO_4)_2(OH)_2{\cdot}6(H_2O,OH)$ → santabarbaraite $Fe_3^{3+}(PO_4)_2(OH)_3{\cdot}$ $5H_2O$ (Chukanov *et al.*, 2012); vivianite → ferrostrunzite Fe^{2+} $Fe_2^{3+}(PO_4)_2(OH)_2{\cdot}5H_2O$ → ferristrunzite Fe^{3+} $Fe_2^{3+}(PO_4)_2(OH)_3{\cdot}5H_2O$ (Frost *et al.*, 2004); triphylite $Li(Fe^{2+},Mn^{2+})(PO_4)$ → ferrisicklerite $Li_x(Fe^{3+},Fe^{2+},Mn^{2+})(PO_4)$ → heterosite $Fe^{3+}(PO_4)$ (Schmid-Beurmann *et al.*, 2012); minerals of the eosphorite–childrenite series $(Mn^{2+},Fe^{2+})Al(PO_4)$ $(OH)_2{\cdot}H_2O$ → ernstite $(Mn^{2+},Fe^{3+},Fe^{2+})Al(PO_4)$ $(OH,O)_2{\cdot}H_2O$ (Scholz *et al.*, 2008); phosphoferrite $Fe^{2+}Fe_2^{2+}(PO_4)_2{\cdot}3H_2O$ → kryzhanovskite Fe^{3+} $Fe_2^{3+}(PO_4)_2(OH)_3$ (Moore and Araki, 1976; Moore *et al.*, 1980). We believe that eleonorite is a transformational mineral species formed as a result of the oxidation of beraunite according to the scheme $Fe^{2+}Fe_5^{3+}(PO_4)_4(OH)_5{\cdot}6H_2O$ → $Fe_6^{3+}(PO_4)_4$ $O(OH)_4{\cdot}6H_2O$. Eleonorite is the twelfth phosphate mineral with only ferric iron as the species-defining metal cation. These minerals belong to different structural types and contain Fe^{3+} with a different coordination number. Crystal data for these minerals are summarized in Table 11.

References

Arnold, H. (1986) Crystal structure of $FePO_4$ at 294 and 20 K. *Zeitschrift für Kristallographie*, **177**, 139–142.

Blanchard, F.N. and Denahan, S.A. (1968) Cacoxenite and beraunite from Florida. *American Mineralogist*, **53**, 2096–2101.

Brandenburg, K. (1999) *DIAMOND, version 2.1c.* Crystal Impact GbR, Bonn, Germany.

Breithaupt, A. (1841) *Vollständiges Handbuch der Mineralogie.* Volume 2. Arnoldische Buchhandlung, Dresden and Leipzig, Germany.

Brown, I.D. (2002) *The Chemical Bond in Inorganic Chemistry. The Bond Valence Model.* Oxford University Press, Oxford, UK.

Brown, I.D. and Altermatt, D. (1985) Bond-valence parameters obtained from a systematic analysis of the inorganic crystal structure database. *Acta Crystallographica*, **B41**, 244–247.

Brown, I.D. and Shannon, R.D. (1973) Empirical bond strength – bond lengths curves for oxides. *Acta Crystallographica*, **A29**, 266–282.

Bruker (2009) *APEX2.* Bruker AXS Inc., Madison, Wisconsin, USA.

Chukanov, N.V. (2014) *Infrared Spectra of Mineral Species: Extended Library.* Springer-Verlag GmbH, Dordrecht, The Netherlands.

Chukanov, N.V., Scholz, R., Aksenov, S.M., Rastsvetaeva, R.K., Pekov, I.V., Belakovskiy, D.I., Krambrock, K., Paniago, R.M., Righi, A., Martins, R. F., Belotti, F.M. and Bermanec, V. (2012) Metavivianite, $Fe^{2+}Fe_2^{3+}(PO_4)_2(OH)_2{\cdot}6H_2O$: new data and formula revision. *Mineralogical Magazine*, **76**, 725–741.

Cipriani, C., Mellini, M., Pratesi, G. and Viti, C. (1997) Rodolicoite and grattarolaite, two new phosphate minerals from Santa Barbara mine, Italy. *European Journal of Mineralogy*, **9**, 1101–1106.

Eventoff, W., Martin, R. and Peacor, D.R. (1972) The crystal structure of heterosite. *American Mineralogist*, **57**, 45–51.

Fanfani, L. and Zanazzi, P.F. (1967) The crystal structure of beraunite. *Acta Crystallographica*, **22**, 173–181.

Frondel, C. (1949) The dufrenite problem. *American Mineralogist*, **34**, 513–540.

Frost, R.L., Weier, M.L. and Lyon, W. (2004) Metavivianite, an intermediate mineral phase between vivianite, and ferro/ferristrunzite. A Raman spectroscopic study. *Neues Jahrbuch für Mineralogie, Monatshefte*, **2004**, 228–240.

Ibers, J.A. and Hamilton, W.C. (1974) *International Tables for X-ray Crystallography.* The Kynoch Press. Birmingham, UK.

Kampf, A.R., Mills, S.J., Nash, B.P., Housley, R. M., Rossman, G.R. and Dini, M. (2013) Camaronesite, $Fe^{3+}(H_2O)_2(PO_3OH))_2(SO_4)\cdot1–2$ (H_2O), a new phosphate-sulfate from the Camarones Valley, Chile, structurally related to taranakite. *Mineralogical Magazine*, **77**, 453–465.

Kolitsch, U., Bernhardt, H.J., Lengauer, C.L., Blass, G. and Tillmanns, E. (2006) Allanpringite, $Fe_3(PO_4)_2(OH)_3\cdot5(H_2O)$, a new ferric iron phosphate from Germany, and its close relation to wavellite. *European Journal of Mineralogy*, **18**, 793–801.

Marzoni Fecia di Cossato, Y., Orlandi, P. and Pasero, M. (1989) Manganese-bearing beraunite from Mangualde, Portugal: mineral data and structure refinement. *The Canadian Mineralogist*, **27**, 441–446.

Modaressi, A., Courtois, A., Gérardin, R., Malaman, B. and Gleitzer, C. (1983) Fe_3PO_7, un cas de coordinence 5 du fer trivalent, étude structurale et magnétique. *Journal of Solid State Chemistry*, **47**, 245–255.

Moore, P.B. (1966) The crystal structure of metastrengite and its relationship to strengite and phosphophyllite. *American Mineralogist*, **51**, 168–176.

Moore, P.B. (1969) The basic ferric phosphates: a crystallochemical principle. *Science*, **164**, 1063–1064.

Moore, P.B. (1970) Crystal chemistry of the basic iron phosphates. *American Mineralogist*, **55**, 135–169.

Moore, P.B. and Araki, T. (1976) A mixed-valence solid-solution series' crystal structures of phosphoferrite, $Fe_3^{(II)}(H_2O)_3(PO_4)_2$, and kryshanovskite, $Fe_3^{(III)}(OH)_3(PO_4)_2$. *Inorganic Chemistry*, **15**, 316–321.

Moore, P.B. and Kampf, A.R. (1992) Beraunite: refinement, comparative crystal chemistry, and selected bond valences. *Zeitschrift für Kristallographie*, **201**, 263–281.

Moore, P.B., Araki, T. and Kampf, A.R. (1980) Nomenclature of the phosphoferrite structure type: refinements of landsite and kryzhanovskite. *Mineralogical Magazine*, **43**, 789–795.

Nies, A. (1877) Strengit, ein neues Mineral. *Neues Jahrbuch für Mineralogie, Geologie und Palaeontologie*, 8–16.

Nies, A. (1880) Vorläufiger Bericht über zwei neue Mineralien von der Grube Eleonore am Dünsberg bei Gießen. *Berichte der Oberhessischen Gesellschaft für Natur- und Heilkunde*, **19**, 111–113.

Palache, C., Berman, H. and Frondel, C. (1951) *The System of Mineralogy of James Dwight Dana and Edward Salisbury Dana.* Volume II. John Wiley and Sons, New York.

Peacor, D.R., Dunn, P.J., Simmons, W.B. and Ramik, R.A. (1987) Ferristrunzite, a new member of the strunzite group, from Blaton, Belgium. *Neues Jahrbuch für Mineralogie, Monatshefte*, 433–440.

Peacor, D.R., Rouse, R.C., Coskren, T.D. and Essene, E.J. (1999) Destinezite ("diadochite"), $Fe_2(PO_4)(SO_4)$ $(OH)\cdot6H_2O$: its crystal structure and role as a soil mineral at Alum Cave Bluff, Tennessee. *Clays and Clay Minerals*, **47**, 1–11.

Petříček, V., Dusek, M. and Palatinus, L. (2006) *Jana2006. Structure Determination Software Programs.* Institute of Physics, Praha, Czech Republic.

Pratesi, G., Cipriani, C., Giuli, G. and Birch, W.D. (2003) Santabarbaraite: a new amorphous phosphate mineral. *European Journal of Mineralogy*, **15**, 185–192.

Rius, J., Louer, D., Louer, M., Gali, S. and Melgarejo, J.C. (2000) Structure solution from powder data of the phosphate hydrate tinticite. *European Journal of Mineralogy*, **12**, 581–588.

Robinson, K., Gibbs, G.V. and Ribbe, P.H. (1971) Quadratic elongation: a quantitative measure of distortion in coordination polyhedra. *Science*, **172**, 567–570.

Sakurai, K., Matsubara, S. and Kato, A. (1987) Koninckite from the Suwa mine, Chino City, Nagano Prefecture, Japan. *Bulletin of the National Science Museum Tokyo, Series C*, **13**, 149–156.

Schmid-Beurmann, P., Ottolini, L., Hatert, F., Geisler, T., Huyskens, M. and Kahl, V. (2012) Topotactic formation of ferrisicklerite from natural triphylite under hydrothermal conditions. *Mineralogy and Petrology*, **107**, 501–515.

Scholz, R., Karfunkel, J., Bermanec, V., Da Costa, G.-M., Horn, A.-H., Cruz Souza, L.-A. and Bilal, E. (2008) Amblygonite-montebrasite from Divino das Laranjeiras – Mendes Pimentel pegmatitic swarm, Minas Gerais Brasil. II. Mineralogy. *Romanian Journal of Mineral Deposits*, **83**, 131–147.

Sejkora, J., Škoda, R., Ondruš, P., Beran, P. and Süsser, C. (2006) Mineralogy of phosphate accumulations in the Huber stock, Krásno ore district, Slavkovský Les area, Czech Republic. *Journal of the Czech Geological Society*, **51/1(2)**, 103–147.

Sejkora, J., Grey, I.E., Kampf, A.R. and Price, J.R. (2015) Tvrdýite, IMA 2014-082. CNMNC Newsletter No. 23, February 2015, page 57; *Mineralogical Magazine*, **79**, 51–58.

Sejkora, J., Grey, I.E., Kampf, A.R., Price, J.R. and Čejka, J. (2016) Tvrdýite, $Fe^{2+}Fe_2^{3+}$ $Al_3(PO_4)_4(OH)_5(OH_2)_4\cdot$ $2H_2O$, a new phosphate mineral from Krásno near Horný Slavkov, Czech Republic. *Mineralogical Magazine*, **80**, 1077–1088.

Shannon, R.D. (1976) Revised effective ionic radii and systematic studies of interatomic distances in halides and chalcogenides. *Acta Crystallographica*, **A64**, 751–767.

Streng, A. (1881) Ueber die Phosphate von Waldgirmes. *Neues Jahrbuch für Mineralogie, Geologie und Palaeontologie*, 101–119.

Taxer, K. and Bartl, H. (2004) On the dimorphy between the variscite and clinovariscite group: refined finestructural relationship of strengite and clinostrengite, Fe (PO$_4$)·2H$_2$O. *Crystal Research and Technology*, **39**, 1080–1088.